

# Probing the Electroweak Sphaleron with Gravitational Waves

Ruiyu Zhou<sup>1</sup>, Ligong Bian<sup>1,\*</sup> and Huai-Ke Guo<sup>2†</sup>

<sup>1</sup> *Department of Physics, Chongqing University, Chongqing 401331, China*

<sup>2</sup> *Department of Physics and Astronomy, University of Oklahoma, Norman, OK 73019, USA*

(Dated: October 2, 2019)

We present the relation between the sphaleron energy and the gravitational wave signals from a first order electroweak phase transition. The crucial ingredient is the scaling law between the sphaleron energy at the temperature of the phase transition and that at zero temperature. We estimate the baryon number preservation criterion, and observe that for a sufficiently strong phase transition, it is possible to probe the electroweak sphaleron using measurements of future space-based gravitational wave detectors.

## I. INTRODUCTION

The observation of gravitational wave signals from the Binary Black hole merger by LIGO [1] and the approval of the space-based interferometer LISA by the European Space Agency [2] have raised increasing interest on the study of gravitational waves from the Electroweak phase transition (EWPT) in the early Universe. To account for the baryon asymmetry of the Universe (BAU), the mechanism of electroweak baryogenesis (EWBG) requires a strongly first order electroweak phase transition (SFOEWPT). The SFOEWPT provides a non-equilibrium environment for baryon number generation [3](see [4, 5] for recent reviews on EWBG and cosmic phase transitions), fulfilling one of the three Sakharov conditions [6]. The (B+L)-violating sphaleron process associated with the change of Chern-Simons numbers [7, 8] should be suppressed to avoid the washout of the baryon asymmetry inside the electroweak bubbles (electroweak broken phase) after the EWPT [3]. Particularly, the sphaleron rate in the broken phase is proportional to a Boltzmann factor  $\Gamma \propto \exp[-E_{sph}(T)/T]$  [3, 9], with here  $E_{sph}(T)$  representing the sphaleron energy (energy barrier) of the saddle-point configuration of the electroweak theory [8]. The requirement that the sphaleron process needs to be sufficiently quenched constrains the possible patterns of EWPT and thus the generated gravitational waves since  $E_{sph}(T)$  is highly correlated with the Higgs VEV at finite temperature as will be

explored in the following. We therefore propose to probe the sphaleron process at the finite temperature through the measurement of the gravitational wave signals.

We start by studying the relation between the sphaleron energy and the strength of the EWPT. Requiring the sphaleron rate in the broken phase to be lower than the Hubble expansion rate results in the baryon number preservation criterion (BNPC) [10]<sup>1</sup>,

$$\frac{E_{sph}(T)}{T} > (35.9 - 42.8) + 7 \ln \frac{v(T)}{T} - \ln \frac{T}{100 \text{ GeV}}, \quad (1)$$

where the numerical range comes from the uncertainty associated with the determination of the fluctuation determinant  $\kappa = (10^{-4} - 10^{-1})$  as adopted by Dine *et al.* [12] and is comparable to the uncertainty in the numerical lattice simulation of the sphalerons at the Standard Model electroweak (EW) crossover [11]. In this work, we calculate  $E_{sph}(T)$  directly and test the BNPC by examining the quantity

$$PT_{sph} = \frac{E_{sph}(T)}{T} - 7 \ln \frac{v(T)}{T} + \ln \frac{T}{100 \text{ GeV}}, \quad (2)$$

at the temperature of the EWPT, which is crucial for guaranteeing a successful baryon asymmetry generation. We use the Standard Effective field theory (SMEFT) and the extensively studied singlet extended Standard Model (“xSM”) as two concrete examples and find that the BNPC condition can set a more rigorous bound on the new physics scale than the conventionally adopted

\* lgbycl@cqu.edu.cn

† ghk@ou.edu

<sup>1</sup> Here, we note that the exact settling down of this relation requires lattice simulation of the sphaleron rate. See Ref. [11] for a recent study in the SM.

SFOEWPT condition [13]:  $\frac{v(T)}{T} \gtrsim 1$ . We then check the scaling law, which states that the sphaleron energy at the temperature of phase transition ( $E_{\text{sph}}(T)$ ) and that at the zero temperature ( $E_{\text{sph}}$ ) obeys an approximate scaling relation [14, 15]:

$$E_{\text{sph}}(T) \approx E_{\text{sph}} \frac{v(T)}{v}, \quad (3)$$

where  $v(T)$  and  $v$  are the VEVs at the time of the phase transition and at zero temperature respectively. Our analysis shows that the scaling law can be established when the strength of the phase transition increases to  $PT_{\text{sph}} \sim \mathcal{O}(10^2)$ , where the SFOEWPT points also meet the BNPC condition. In this scenario, one usually has a smaller  $\beta/H_n$  accompanied with a larger  $\alpha$ , and therefore a higher magnitude of the gravitational wave spectra, as shown in Section II B, which allows us to build a connection between the sphaleron energy and the gravitational wave spectra measurements.

## II. EWPT, GRAVITATIONAL WAVES AND SPHALERONS

### A. The models

It is well known that the SM can not accommodate a first order EWPT and this has motivated a plethora of beyond the standard model scenarios with an extended Higgs sector. From an effective field theory point of view, a first order EWPT can be realized by inclusion of higher dimensional operators, irrespective of a specific scenario. Among the dimension-six operators of the SMEFT, the operator  $O_6$  dominates the contribution to the Higgs potential. Defining the SM Higgs doublet as  $H^T = (G^+, (v+h+iG^0)/\sqrt{2})$ , we then have the following scalar potential:

$$V(H) = -m^2(H^\dagger H) + \lambda(H^\dagger H)^2 + \frac{(H^\dagger H)^3}{\Lambda^2}. \quad (4)$$

The presence of the last term allows the electroweak phase transition to be first order [16, 17], since taking  $\mu^2 > 0$  and  $\lambda < 0$  leads to a potential with a barrier between two minima. The minimization condition and the

Higgs mass definition lead to the relation

$$m^2 = \frac{1}{2}m_h^2 - \frac{3}{4}\frac{v^4}{\Lambda^2}, \quad \lambda = \frac{m_h^2}{2v^2} - \frac{3}{2}\frac{v^2}{\Lambda^2}. \quad (5)$$

To study the EWPT, we need the finite temperature effective potential, which is given by<sup>2</sup>

$$V_T(h, T) = V(h) + \frac{1}{2}c_{hT}h^2, \quad (6)$$

where  $c_{hT} = (4y_t^2 + 3g^2 + g'^2 + 8\lambda)T^2/16$ . The requirement of the EW minimum being the global one results in the condition  $\Lambda \geq v^2/m_h$ , and the EWPT can be first order when the potential barrier can be raised with  $\Lambda < \sqrt{3}v^2/m_h$  [16, 27].

Going beyond the framework of the SMEFT, a simplified benchmark model is the gauge singlet extension of the SM, known as the “xSM”, with the potential defined by [22, 23, 25],

$$V(H, S) = -m^2 H^\dagger H + \lambda(H^\dagger H)^2 + \frac{a_1}{2} H^\dagger H S + \frac{a_2}{2} H^\dagger H S^2 + \frac{b_2}{2} S^2 + \frac{b_3}{3} S^3 + \frac{b_4}{4} S^4,$$

where  $S = v_s + s$  is the real scalar gauge singlet. The finite temperature potential is [28]:

$$V[h, s, T] = -\frac{1}{2}[m^2 - \Pi_h[T]]h^2 - \frac{1}{2}[-b_2 - \Pi_s[T]]s^2 + \frac{1}{4}\lambda h^4 + \frac{1}{4}a_1 h^2 s + \frac{1}{4}a_2 h^2 s^2 + \frac{b_3}{3}s^3 + \frac{b_4}{4}s^4, \quad (7)$$

where  $\Pi_h(T)$  and  $\Pi_s$  are the thermal masses of the fields,

$$\begin{aligned} \Pi_h[T] &= \left( \frac{2m_W^2 + m_Z^2 + 2m_t^2}{4v^2} + \frac{\lambda}{2} + \frac{a_2}{24} \right) T^2, \\ \Pi_s[T] &= \left( \frac{a_2}{6} + \frac{b_4}{4} \right) T^2. \end{aligned} \quad (8)$$

The scalar cubic terms in Eq. 7 dominate the phase transition dynamics and can accommodate a first order EWPT after theoretical and experimental bounds on model parameters are taken into account. Moreover, in this work, we focus on the one-step EWPT with the EW vacuum denoted by ( $\equiv (v, v_s)$ ), though two-step EWPT can also exist, which however is of negligible parameter space here [28].

<sup>2</sup> In the standard approach, one includes the tree level effective potential, the Coleman-Weinberg term [18] and its finite temperature counterpart [13], together with the daisy resummation [19, 20]. For the EWPT mainly driven by the cubic terms in the potential, and with a purpose of maintaining a gauge independent effective potential [21], we use the gauge invariant high temperature expansion approximation [22–26].

## B. Gravitational Waves

With the finite temperature effective potential given above, the Higgs VEV at finite temperature ( $v(T)$ ) can be obtained. Here and in the following sections we define the temperature of the EWPT as  $T_* \approx T_n$ <sup>3</sup>, with  $T_n$  being the bubble nucleation temperature. The phase transition order parameter  $v_n/T_n$  (the phase transition strength at the bubble nucleation temperature) and the two crucial parameters for the GW spectrum from the EWPT are calculated using **CosmoTransitions** [30]. The first parameter crucial for the GW spectrum is the ratio of released latent heat from the transition to the total radiation energy density [29]

$$\alpha = \frac{1}{\rho_R} \left[ -(V_{\text{EW}} - V_f) + T \left( \frac{dV_{\text{EW}}}{dT} - \frac{dV_f}{dT} \right) \right] \Big|_{T=T_*}, \quad (9)$$

where  $V_f$  is the value of the potential at the metastable vacuum and  $V_{\text{EW}}$  is that in the EW vacuum. Another parameter  $\beta/H_n$  serves as a time scale for the EWPT:

$$\frac{\beta}{H_n} = \left[ T \frac{d}{dT} \left( \frac{S_3(T)}{T} \right) \right] \Big|_{T=T_*}, \quad (10)$$

where  $H_n$  is the Hubble rate at  $T_n$  and  $S_3(T)$  the action for the  $O(3)$  symmetric bounce action.

The dominant sources for GW production during the EWPT are the sound waves in the plasma [31, 32] and the magnetohydrodynamic turbulence (MHD) [31, 32]<sup>4</sup>. To a good approximation, the total energy density of the gravitational waves in unit of the critical energy density of the universe is given by [29]

$$\Omega_{\text{GW}}(f)h^2 \approx \Omega_{\text{sw}}(f)h^2 + \Omega_{\text{turb}}(f)h^2. \quad (11)$$

Due to its stochastic nature, this kind of gravitational waves can be searched for by cross-correlating outputs from two or more detectors, with the resulting signal-to-noise ratio(SNR) obtained as [29]

$$\text{SNR} = \sqrt{\mathcal{T} \int df \left[ \frac{h^2 \Omega_{\text{GW}}(f)}{h^2 \Omega_{\text{exp}}(f)} \right]^2}, \quad (12)$$

<sup>3</sup> The approximation is justified for a EWPT without significant reheating [29]

<sup>4</sup> We neglect here the contribution from the bubble wall collisions [33–38], as it is now generally believed to be negligible [39].

where  $\mathcal{T}$  is the duration of the data in years and  $\Omega_{\text{exp}}$  the power spectral density of the detector.

As shown in Appendix. A, the  $\Omega_{\text{GW}}(f)h^2$  is proportional to  $\beta/H_n$ , which has generally small values and is accompanied with a relatively large  $\alpha$  for a strong phase transitions (a higher value of  $v_n/T_n$ ) [28, 40]. Generally, one has  $\alpha$  growing as  $\Delta V \equiv (V_{\text{EW}} - V_f)$  and  $\beta/H_n$  scaling as  $1/\sqrt{\Delta V}$  for a given finite temperature potential [41]. This makes it possible to connect the sphaleron energy with the GW measurements since  $E_{\text{sph}}(T_n)$  is proportional to  $v_n/T_n$ , and a large  $v_n/T_n$  corresponds to a highly suppressed sphaleron rate inside the EW vacuum bubble as will be explored below.

## C. The Electroweak Sphaleron

The electroweak sphaleron is a static but unstable solution to the classical equations of motion of the EW theory, which corresponds to a saddle-point configuration in the field space and sits at the top of the potential barrier between two topologically distinct vacua with adjacent values of the Chern-Simons number [7, 8]. To calculate the energy of the sphaleron configuration, we adopt the spherically symmetric ansatz since the  $U(1)_Y$  contribution is sufficiently small [8, 42–44]. In the xSM, it follows that

$$\begin{aligned} E_{\text{sph}}(T) = & \frac{4\pi\Omega[T]}{g} \int_0^\infty d\xi \left[ 4 \left( \frac{df}{d\xi} \right)^2 \right. \\ & + \frac{8}{\xi^2} f^2 (1-f)^2 + \frac{\xi^2 v[T]^2}{2\Omega[T]^2} \left( \frac{dh}{d\xi} \right)^2 \\ & + \frac{v[T]^2}{\Omega[T]^2} (1-f)^2 h^2 + \frac{\xi^2 v_s[T]^2}{2\Omega[T]^2} \left( \frac{dk}{d\xi} \right)^2 \\ & \left. + \frac{\xi^2}{g^2 \Omega[T]^4} (V_{\text{eff}}[h, k, T]) \right], \end{aligned} \quad (13)$$

where  $h, f, k$  are field configurations defined in Appendix B,  $\xi = g_2 \Omega[T] r$ , and  $V_{\text{eff}}[h, k, T] = V[h, k, T] - \Delta[T]$ , with  $\Delta[T]$  being the cosmological constant energy density which can be regarded as the minimal value of the potential at temperature  $T$  [45]. Here  $4\pi v[T]/g$  has the unit of energy and the integral gives a dimensionless number;  $\Omega[T]$  can take any non-vanishing value of mass dimension one (for example  $v[T]$ ,  $v_S[T]$

or  $\sqrt{v[T]^2 + v_S[T]^2}$ ;  $v[T], v_S[T]$  are the VEVs of  $h, s$  at temperature  $T$  and  $v[T] = v, v_S[T] = v_S$  at  $T = 0$ . When the singlet part is absent, the above  $E_{\text{sph}}(T)$  reduces to the form of the SMEFT case, with the potential:

$$V_{\text{eff}}[h, T] = V_T(h, T) - V_T(v(T), T). \quad (14)$$

For more details on the field configurations and on the sphaleron solutions, see Appendix. B. The sphaleron energy at the bubble nucleation temperature  $T_n(E_{\text{sph}}(T_n))$  can be obtained after the parameters  $v(T_n), v_S(T_n)$  and  $T_n$  have been calculated through the EWPT analysis.

### III. RESULTS

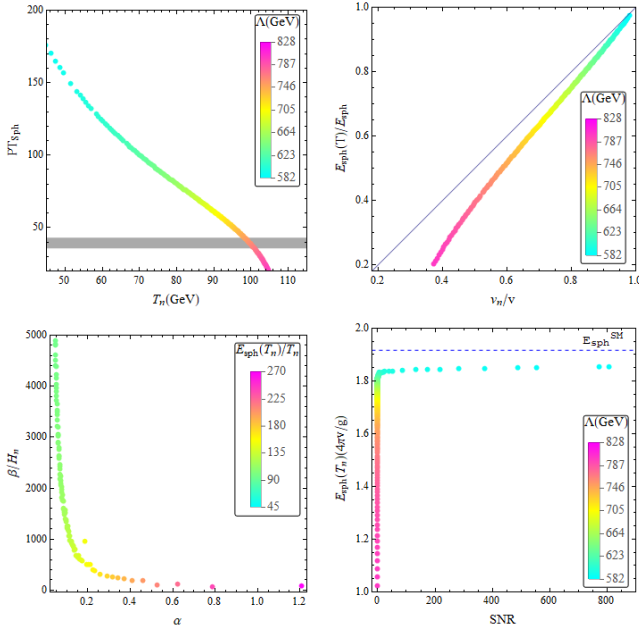


Figure 1. In the top panels, we plot  $PT_{\text{sph}}$  versus  $T_n$  (left), and  $E_{\text{sph}}(T_n)/E_{\text{sph}}$  versus  $v_n/v$  (right) when varying  $\Lambda$  for the case of the SMEFT. The bottom panels show  $\beta/H_n$  versus  $\alpha$  by color-coding  $E_{\text{sph}}(T_n)/T_n$  (left), and the relation between the sphaleron energy  $E_{\text{sph}}(T_n)$  and the SNR of the GW spectra (right).

In the top panel of Fig. 1, we first present the relation between the BNPC and the new physics scale, where the horizontal shaded region represents the uncertainty of  $\kappa$  in the sphaleron rate, i.e. the range  $[35.9, 42.8]$  in Eq.1 (this corresponds to  $749 < \Lambda < 768$  GeV). When  $PT_{\text{sph}}$  is above this region, the BNPC is satisfied, while

$v_n/T_n \geq 1$  is obtained when  $\Lambda < 790$  GeV. The top-right panel demonstrates the scaling law, where the deviation from the scaling law becomes smaller when the phase transition strength becomes larger obtained with a lower new physics scale  $\Lambda$ . We further present the relation between  $E_{\text{sph}}(T_n)/T_n$  and the gravitational wave parameters  $\alpha$  and  $\beta/H_n$  in the bottom left panel. This demonstrates that a larger  $\alpha$  (with a larger phase transition strength  $v_n/T_n$ ) and a smaller  $\beta/H_n$  generally lead to a larger  $E_{\text{sph}}(T_n)/T_n$ , for which the sphaleron rate is highly suppressed and washout of the baryon asymmetry can be avoided. This correlation among these parameters is anticipated, as a larger  $v_n$  can generally be obtained with a more significant supercooling. The relation between the sphaleron energy and the SNR of the corresponding gravitational wave spectra from the EWPT is shown in the bottom-right plot, which indicates that the sphaleron can be probed by the gravitational wave detector (with a larger SNR) when  $\Lambda$  is lower. The  $E_{\text{sph}}(T_n)/T_n$  obtained for all EWPT points are smaller than the SM sphaleron energy at zero temperature.

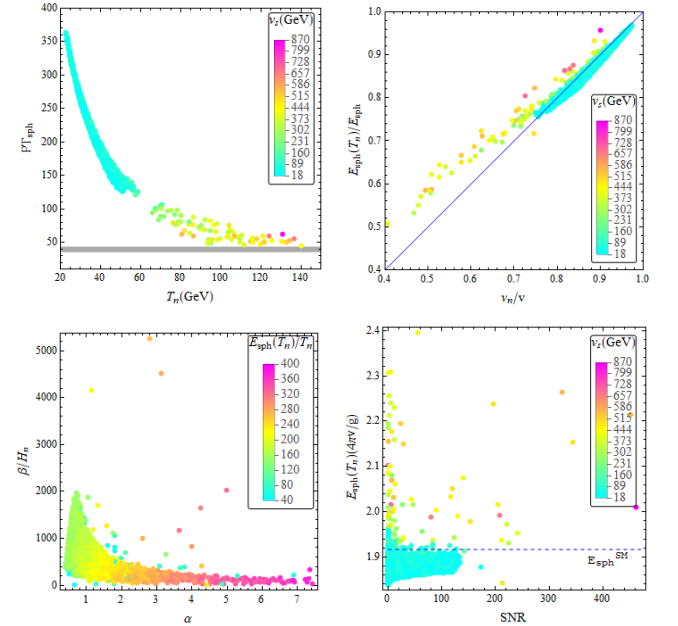


Figure 2. As in Fig. 1, we show similar plots with  $v_n/T_n > 1$  and  $\text{SNR} > 10$ , where  $v_s$  is the VEV of the singlet at zero temperature.

Now we move to another scenario, where the new

physics that is necessary for a first order EWPT cannot be integrated out. We illustrate the situation with the xSM (see Ref.[27, 46] for the mismatch between the SMEFT and xSM model), and show in Fig.2 the points with  $\text{SNR} > 10$ . The top-left panel of Fig.2 shows that a lower  $v_s$  generally leads to a lower  $T_n$  and a larger  $PT_{sph}$ . The top-right panel shows that the scaling law is better satisfied for small  $v_s$ . We then examine the relation between  $E_{sph}(T_n)/T_n$  and  $(\alpha, \beta/H_n)$  in the bottom-left panel, which indicates a similar behavior as the SMEFT case. The bottom-right panel shows that the sphaleron energy is concentrated at around 1.9 (in unit of  $4\pi v/g$ ) for small  $v_s$ , where the GW signal can be probed by LISA [29]. In the SNR calculation for the SFOEWPT points, we include the deficit found in the GW production from the sound waves [47]<sup>5</sup>. The  $E_{sph}(T_n)/T_n$  for most SFOEWPT points are found to be smaller than the SM sphaleron energy at zero temperature.

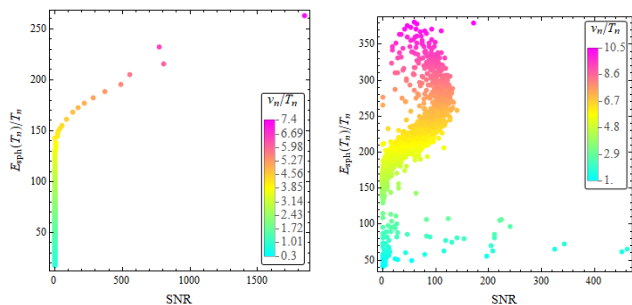


Figure 3. We show the SNR of the GW spectra versus the  $E_{sph}/T_n$  by color-coding  $v_n/T_n$  for SMEFT (left panel) and xSM (right panel).

We finally present Fig. 3, which shows that a EWPT which is strong enough to produce an observable gravitational wave signal can effectively “switch off” the sphaleron rate after the transition as required by the

EWBG.

#### IV. CONCLUSIONS AND DISCUSSION

We have calculated the energy of the electroweak sphaleron during the EWPT and revealed the relation between the BNPC and the new physics scale using the SMEFT and xSM as two concrete examples. The scaling law can be established approximately when there is a higher phase transition strength associated with a lower new physics scale. In this scenario, it is possible to use the GW detectors to access the sphaleron energy, thus providing an alternative way of probing the sphaleron in addition to the high energy colliders<sup>6</sup>. Different from other sources of the gravitational waves such as cosmic strings, domain walls, and primordial black hole, the GWs from SFOEWPT can also be tested through future colliders, since the SFOEWPT usually is accompanied by a deviation of the triple and quartic Higgs couplings in the Higgs potential<sup>7</sup>. Thus the relation between the sphaleron energy and the phase transition strength studied here makes it possible to probe the sphaleron through both gravitational wave and collider measurements, in a complementary role.

At last, we note that our findings in this work rely only mildly on the numerical uncertainty in Eq. 1. Settling down the numerical range for a specific particle physics model would require a lattice simulation of the sphaleron rate [60]<sup>8</sup>.

<sup>5</sup> Note that the results of a recent numerical simulation by the same group shows that for strong EWPT (i.e., those with  $\alpha \sim 1$ ), there is a significant deficit in the GW production from the sound waves [47]. This invalidates the naive generalization of the GW formulae to arbitrary values of  $(v_w, \alpha)$ . For the xSM, this leads to a shrinking of the parameter space that gives detectable GWs while the main features of the resulting parameter space remains qualitatively unchanged (see [48] for a detailed study). For the SMEFT, however, it leads to a more severe reduction of the parameter space, making it difficult to generate detectable GWs.

<sup>6</sup> Probing the (B+L)-violation process is of crucial importance to test the Sakharov conditions and the EWBG mechanism. Previously, the conventional wisdom is that the (B+L)-violating process at zero temperature is difficult to probe at current and near future high energy colliders as the sphaleron induced (B+L)-violating process is highly rare [9, 49–52]. Very recently, the Bloch wave approach was proposed such that there is a chance to observe a (B+L)-violating event at the Large Hadron Collider (LHC) [53–57].

<sup>7</sup> The sensitivities of future colliders in the SFOEWPT parameter space (where one can have gravitational wave signal) can be accessed with the measurements of the two couplings ( $\lambda_{hhh}$  and  $\lambda_{hhhh}$ ) at future  $e^+e^-$  colliders and the HL-LHC [58, 59].

<sup>8</sup> The starting point of the lattice simulation of the sphaleron rate and EWPT is the dimensional reduction. For the SMEFT theory with dimensional six operators, the 3d EFT obtained after dimensional reduction is not super-renormalizable, and the lattice-continuum relations receive corrections at all orders in

## ACKNOWLEDGMENTS

The work of L.B. is supported by the National Natural Science Foundation of China under grant No.11605016 and No.11647307. H.G. is partially supported by the U.S. Department of Energy grant de-sc0009956. We thank F.R. Klinkhamer, Mark Hindmarsh, Salah Nasri, Guy D. Moore, Mikko Laine, Lauri Niemi, Kari Rummukainen, Lian-Tao Wang, Koichi Funakubo, and Heng-Tong Ding for helpful communications and discussions.

## Appendix A: The GW Energy Density Spectra

It is realized in recent years that the long lasting sound waves in the plasma during and after the phase transition constitutes the dominant GW source [31, 32]. The energy density spectrum from this source is obtained by large scale numerical simulations, based on the scalar field and fluid model, for weak phase transitions corresponding to small values of  $v_w$  and  $\alpha$ . It is well fitted by [32]

$$\Omega_{\text{sw}} h^2 = 2.65 \times 10^{-6} \left( \frac{H_*}{\beta} \right) \left( \frac{\kappa_v \alpha}{1 + \alpha} \right)^2 \left( \frac{100}{g_*} \right)^{1/3} v_w \left( \frac{f}{f_{\text{sw}}} \right)^3 \left( \frac{7}{4 + 3(f/f_{\text{sw}})^2} \right)^{7/2}, \quad (\text{A1})$$

where  $H_*$  is the Hubble rate at  $T_*$  when the phase transition finished, which is only slightly different from  $T_n$ ;  $v_w$  is the bubble wall velocity and is chosen so that a non-relativistic relative velocity in the bubble wall frame can be obtained to make sure the slower baryon generation process is feasible [28, 48, 66];  $g_*$  is the relativistic degrees of freedom. The factor  $\kappa_v$  denotes the fraction of released energy density that is transferred into the kinetic energy of the plasma, which can be calculated given inputs of  $v_w$  and  $\alpha$  from a hydrodynamic analysis [67]. Moreover  $f_{\text{sw}}$  is the peak frequency:

$$f_{\text{sw}} = 1.9 \times 10^{-5} \frac{1}{v_w} \left( \frac{\beta}{H_*} \right) \left( \frac{T_*}{100 \text{ GeV}} \right) \left( \frac{g_*}{100} \right)^{1/6} \text{ Hz}. \quad (\text{A2})$$

---

perturbation theory. To study the system at small lattice spacings, the difficulty is the determination of the non-perturbative relation between physical inputs and quantities measured on the lattice [61–65]).

We note that the above formulae is limited to relatively small values of  $v_w$  and  $\alpha$ . Recent numerical simulations exploring larger values of  $\alpha$  shows a deficit in the GW production [47](see [48] for a more detailed discussion on the implications of this effect).

There is also a small fraction of energy going to the MHD, with a result that can be fitted by [68, 69]

$$\Omega_{\text{turb}} h^2 = 3.35 \times 10^{-4} \left( \frac{H_*}{\beta} \right) \left( \frac{\kappa_{\text{turb}} \alpha}{1 + \alpha} \right)^{3/2} \left( \frac{100}{g_*} \right)^{1/3} v_w \frac{(f/f_{\text{turb}})^3}{[1 + (f/f_{\text{turb}})]^{11/3} (1 + 8\pi f/h_*)}, \quad (\text{A3})$$

where  $\kappa_{\text{turb}}$  is the fraction of the energy transferred to the MHD turbulence and is approximately given by  $\kappa_{\text{turb}} \approx (0.05 \sim 0.1) \kappa_v$ . We take here  $\epsilon \approx 0.1$ . Finally  $f_{\text{turb}}$  is the peak frequency this spectrum:

$$f_{\text{turb}} = 2.7 \times 10^{-5} \frac{1}{v_w} \left( \frac{\beta}{H_*} \right) \left( \frac{T_*}{100 \text{ GeV}} \right) \left( \frac{g_*}{100} \right)^{1/6} \text{ Hz}. \quad (\text{A4})$$

## Appendix B: Sphaleron configurations

For the xSM model, we consider the following sphaleron field ansatz [70]:

$$A_i(\mu, r, \theta, \phi) = -\frac{i}{g} f(r) \partial_i U(\mu, \theta, \phi) U^{-1}(\mu, \theta, \phi), \quad (\text{B1})$$

$$H(\mu, r, \theta, \phi) = \frac{v(T)}{\sqrt{2}} \left[ (1 - h(r)) \begin{pmatrix} 0 \\ e^{-i\mu} \cos \mu \end{pmatrix} + h(r) U(\mu, \theta, \phi) \begin{pmatrix} 0 \\ 1 \end{pmatrix} \right], \quad (\text{B2})$$

$$S(\mu, r, \theta, \phi) = v_S(T) k(r), \quad (\text{B3})$$

where  $A_i$  are SU(2) gauge fields, and the matrix  $U$  is defined as

$$U(\mu, \theta, \phi) = \begin{pmatrix} e^{i\mu}(c_\mu - i s_\mu c_\theta) & e^{i\phi} s_\mu s_\theta \\ -e^{-i\phi} s_\mu s_\theta & e^{-i\mu}(c_\mu + i s_\mu c_\theta) \end{pmatrix}, \quad (\text{B4})$$

where the  $s_{\mu(\theta)} = \sin \mu(\theta)$  and  $c_{\mu(\theta)} = \cos \mu(\theta)$ . The sphaleron energy is obtained for  $\mu = \pi/2$  [8]. From

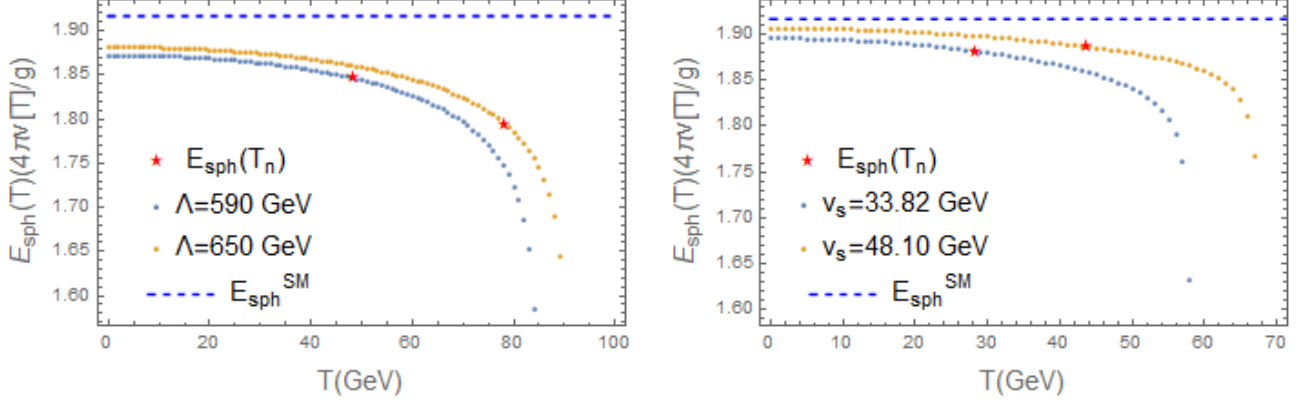


Figure 4. Left:  $E_{sph}(T_n)$  versus  $T$  for the SMEFT,  $SNR = 175(0.002)$  and  $v_n/T_n = 4.8(2.6)$  for  $\Lambda = 590(650)$  GeV; Right: xSM scenario for  $v_s = 33.82(48.10)$  GeV, with  $v_n/T_n = 8.3(5.1)$  and  $SNR = 98(11)$ .

Eq. (13), the equations of motion can be found:

$$\frac{d^2 f}{d\xi^2} = \frac{2}{\xi^2} f(1-f)(1-2f) - \frac{v[T]^2 h^2}{4\Omega[T]^2} (1-f), \quad (B5)$$

$$\frac{d}{d\xi} \left( \xi^2 \frac{dh}{d\xi} \right) = 2h(1-f)^2 + \frac{\xi^2}{g^2} \frac{1}{v[T]^2 \Omega[T]^2} \frac{\partial V_{\text{eff}}(h, k, T)}{\partial h}, \quad (B6)$$

$$\frac{d}{d\xi} \left( \xi^2 \frac{dk}{d\xi} \right) = \frac{\xi^2}{g^2} \frac{1}{v_s[T]^2 \Omega[T]^2} \frac{\partial V_{\text{eff}}(h, k, T)}{\partial k}. \quad (B7)$$

The sphaleron solutions can be obtained with the following boundary conditions,

$$\lim_{\xi \rightarrow 0} f(\xi) = 0, \lim_{\xi \rightarrow 0} h(\xi) = 0, \lim_{\xi \rightarrow 0} k'(\xi) = 0, \\ \lim_{\xi \rightarrow \infty} f(\xi) = 1, \lim_{\xi \rightarrow \infty} h(\xi) = 1, \lim_{\xi \rightarrow \infty} k(\xi) = 1. \quad (B8)$$

For the SMEFT, the sphaleron solutions can be ob-

tained from:

$$\frac{d^2 f}{d\xi^2} = \frac{2}{\xi^2} f(1-f)(1-2f) - \frac{1}{4} h^2 (1-f), \\ \frac{d}{d\xi} \left( \xi^2 \frac{dh}{d\xi} \right) = 2h(1-f)^2 + \frac{\xi^2}{g^2} \frac{1}{v[T]^4} \frac{\partial V_{\text{eff}}(h, T)}{\partial h}, \quad (B9)$$

with boundary conditions given by,

$$\lim_{\xi \rightarrow 0} f(\xi) = 0, \quad \lim_{\xi \rightarrow 0} h(\xi) = 0, \\ \lim_{\xi \rightarrow \infty} f(\xi) = 1, \quad \lim_{\xi \rightarrow \infty} h(\xi) = 1. \quad (B10)$$

We implement the relaxation method as documented in *Numerical Recipes* [71] to solve the above ordinary differential equations numerically.

Here we present Fig. 4 to illustrate that the sphaleron energy at the temperature of the phase transition approaches the corresponding value at the zero temperature when one has a lower  $\Lambda$  for SMEFT (or  $v_s$  in xSM scenario), accompanied with a higher value of the phase transition strength and a larger SNR of the GW spectra. The value  $E_{sph}(T)$  grows as the temperature of the universe decreases, and thus we have an increasingly suppressed sphaleron rate inside the electroweak bubbles after the EWPT.

- 
- [1] **LIGO Scientific, Virgo** Collaboration, B. P. Abbott *et al.*, “Observation of Gravitational Waves from a Binary Black Hole Merger,” *Phys. Rev. Lett.* **116** no. 6, (2016) 061102, [arXiv:1602.03837 \[gr-qc\]](#).  
 [2] **eLISA** Collaboration, P. A. Seoane *et al.*, “The

- Gravitational Universe,” [arXiv:1305.5720 \[astro-ph.CO\]](#).  
 [3] V. A. Kuzmin, V. A. Rubakov, and M. E. Shaposhnikov, “On the Anomalous Electroweak Baryon Number Nonconservation in the Early Universe,” *Phys.*

- Lett.* **155B** (1985) 36.
- [4] D. E. Morrissey and M. J. Ramsey-Musolf, “Electroweak baryogenesis,” *New J. Phys.* **14** (2012) 125003, [arXiv:1206.2942 \[hep-ph\]](#).
  - [5] A. Mazumdar and G. White, “Review of cosmic phase transitions: their significance and experimental signatures,” *Rept. Prog. Phys.* **82** no. 7, (2019) 076901, [arXiv:1811.01948 \[hep-ph\]](#).
  - [6] A. D. Sakharov, “Violation of CP Invariance, C asymmetry, and baryon asymmetry of the universe,” *Pisma Zh. Eksp. Teor. Fiz.* **5** (1967) 32–35. [*Usp. Fiz. Nauk*161,no.5,61(1991)].
  - [7] N. S. Manton, “Topology in the Weinberg-Salam Theory,” *Phys. Rev.* **D28** (1983) 2019.
  - [8] F. R. Klinkhamer and N. S. Manton, “A Saddle Point Solution in the Weinberg-Salam Theory,” *Phys. Rev.* **D30** (1984) 2212.
  - [9] V. A. Rubakov and M. E. Shaposhnikov, “Electroweak baryon number nonconservation in the early universe and in high-energy collisions,” *Usp. Fiz. Nauk* **166** (1996) 493–537, [arXiv:hep-ph/9603208 \[hep-ph\]](#). [*Phys. Usp.*39,461(1996)].
  - [10] X. Gan, A. J. Long, and L.-T. Wang, “Electroweak sphaleron with dimension-six operators,” *Phys. Rev.* **D96** no. 11, (2017) 115018, [arXiv:1708.03061 \[hep-ph\]](#).
  - [11] M. D’Onofrio, K. Rummukainen, and A. Tranberg, “Sphaleron Rate in the Minimal Standard Model,” *Phys. Rev. Lett.* **113** no. 14, (2014) 141602, [arXiv:1404.3565 \[hep-ph\]](#).
  - [12] M. Dine, P. Huet, and R. L. Singleton, Jr., “Baryogenesis at the electroweak scale,” *Nucl. Phys.* **B375** (1992) 625–648.
  - [13] M. Quiros, “Finite temperature field theory and phase transitions,” in *Proceedings, Summer School in High-energy physics and cosmology: Trieste, Italy, June 29-July 17, 1998*, pp. 187–259. 1999. [arXiv:hep-ph/9901312 \[hep-ph\]](#).
  - [14] S. Braibant, Y. Brihaye, and J. Kunz, “Sphalerons at finite temperature,” *Int. J. Mod. Phys.* **A8** (1993) 5563–5574, [arXiv:hep-ph/9302314 \[hep-ph\]](#).
  - [15] Y. Brihaye and J. Kunz, “Electroweak bubbles and sphalerons,” *Phys. Rev.* **D48** (1993) 3884–3890, [arXiv:hep-ph/9304256 \[hep-ph\]](#).
  - [16] C. Grojean, G. Servant, and J. D. Wells, “First-order electroweak phase transition in the standard model with a low cutoff,” *Phys. Rev.* **D71** (2005) 036001, [arXiv:hep-ph/0407019 \[hep-ph\]](#).
  - [17] C. Delaunay, C. Grojean, and J. D. Wells, “Dynamics of Non-renormalizable Electroweak Symmetry Breaking,” *JHEP* **04** (2008) 029, [arXiv:0711.2511 \[hep-ph\]](#).
  - [18] S. R. Coleman and E. J. Weinberg, “Radiative Corrections as the Origin of Spontaneous Symmetry Breaking,” *Phys. Rev.* **D7** (1973) 1888–1910.
  - [19] R. R. Parwani, “Resummation in a hot scalar field theory,” *Phys. Rev.* **D45** (1992) 4695, [arXiv:hep-ph/9204216 \[hep-ph\]](#). [Erratum: *Phys. Rev.*D48,5965(1993)].
  - [20] D. J. Gross, R. D. Pisarski, and L. G. Yaffe, “QCD and Instantons at Finite Temperature,” *Rev. Mod. Phys.* **53** (1981) 43.
  - [21] H. H. Patel and M. J. Ramsey-Musolf, “Baryon Washout, Electroweak Phase Transition, and Perturbation Theory,” *JHEP* **07** (2011) 029, [arXiv:1101.4665 \[hep-ph\]](#).
  - [22] S. Profumo, M. J. Ramsey-Musolf, and G. Shaughnessy, “Singlet Higgs phenomenology and the electroweak phase transition,” *JHEP* **08** (2007) 010, [arXiv:0705.2425 \[hep-ph\]](#).
  - [23] S. Profumo, M. J. Ramsey-Musolf, C. L. Wainwright, and P. Winslow, “Singlet-catalyzed electroweak phase transitions and precision Higgs boson studies,” *Phys. Rev.* **D91** no. 3, (2015) 035018, [arXiv:1407.5342 \[hep-ph\]](#).
  - [24] A. V. Kotwal, M. J. Ramsey-Musolf, J. M. No, and P. Winslow, “Singlet-catalyzed electroweak phase transitions in the 100TeV frontier,” *Phys. Rev.* **D94** no. 3, (2016) 035022, [arXiv:1605.06123 \[hep-ph\]](#).
  - [25] T. Huang, J. M. No, L. Perni, M. Ramsey-Musolf, A. Safonov, M. Spannowsky, and P. Winslow, “Resonant di-Higgs boson production in the  $b\bar{b}WW$  channel: Probing the electroweak phase transition at the LHC,” *Phys. Rev.* **D96** no. 3, (2017) 035007, [arXiv:1701.04442 \[hep-ph\]](#).
  - [26] A. Alves, T. Ghosh, H.-K. Guo, and K. Sinha, “Resonant Di-Higgs Production at Gravitational Wave Benchmarks: A Collider Study using Machine Learning,” *JHEP* **12** (2018) 070, [arXiv:1808.08974 \[hep-ph\]](#).
  - [27] P. Huang, A. Joglekar, B. Li, and C. E. M. Wagner, “Probing the Electroweak Phase Transition at the LHC,” *Phys. Rev.* **D93** no. 5, (2016) 055049, [arXiv:1512.00068 \[hep-ph\]](#).
  - [28] A. Alves, T. Ghosh, H.-K. Guo, K. Sinha, and D. Vagie, “Collider and Gravitational Wave Complementarity in Exploring the Singlet Extension of the Standard Model,” *JHEP* **04** (2019) 052, [arXiv:1812.09333 \[hep-ph\]](#).
  - [29] C. Caprini *et al.*, “Science with the space-based interferometer eLISA. II: Gravitational waves from cosmological phase transitions,” *JCAP* **1604** no. 04, (2016) 001, [arXiv:1512.06239 \[astro-ph.CO\]](#).
  - [30] C. L. Wainwright, “CosmoTransitions: Computing Cosmological Phase Transition Temperatures and Bubble Profiles with Multiple Fields,” *Comput. Phys. Commun.* **183** (2012) 2006–2013, [arXiv:1109.4189 \[hep-ph\]](#).
  - [31] M. Hindmarsh, S. J. Huber, K. Rummukainen, and D. J. Weir, “Gravitational waves from the sound of a first order phase transition,” *Phys. Rev. Lett.* **112** (2014) 041301, [arXiv:1304.2433 \[hep-ph\]](#).
  - [32] M. Hindmarsh, S. J. Huber, K. Rummukainen, and D. J. Weir, “Numerical simulations of acoustically generated gravitational waves at a first order phase transition,” *Phys. Rev.* **D92** no. 12, (2015) 123009, [arXiv:1504.03291 \[astro-ph.CO\]](#).
  - [33] A. Kosowsky, M. S. Turner, and R. Watkins, “Gravitational radiation from colliding vacuum bubbles,” *Phys. Rev.* **D45** (1992) 4514–4535.
  - [34] A. Kosowsky, M. S. Turner, and R. Watkins, “Gravitational waves from first order cosmological phase transitions,” *Phys. Rev. Lett.* **69** (1992) 2026–2029.
  - [35] A. Kosowsky and M. S. Turner, “Gravitational radiation from colliding vacuum bubbles: envelope approximation to many bubble collisions,” *Phys. Rev.* **D47** (1993) 4372–4391, [arXiv:astro-ph/9211004 \[astro-ph\]](#).
  - [36] S. J. Huber and T. Konstandin, “Gravitational Wave Production by Collisions: More Bubbles,” *JCAP* **0809**



- (2008) 022, [arXiv:0806.1828 \[hep-ph\]](#).
- [37] R. Jinno and M. Takimoto, “Gravitational waves from bubble collisions: An analytic derivation,” *Phys. Rev. D* **95** no. 2, (2017) 024009, [arXiv:1605.01403 \[astro-ph.CO\]](#).
- [38] R. Jinno and M. Takimoto, “Gravitational waves from bubble dynamics: Beyond the Envelope,” *JCAP* **1901** (2019) 060, [arXiv:1707.03111 \[hep-ph\]](#).
- [39] D. Bodeker and G. D. Moore, “Can electroweak bubble walls run away?,” *JCAP* **0905** (2009) 009, [arXiv:0903.4099 \[hep-ph\]](#).
- [40] L. Bian, H.-K. Guo, Y. Wu, and R. Zhou, “Gravitational wave and Collider searches for the EWSB patterns,” [arXiv:1906.11664 \[hep-ph\]](#).
- [41] C. Grojean and G. Servant, “Gravitational Waves from Phase Transitions at the Electroweak Scale and Beyond,” *Phys. Rev. D* **75** (2007) 043507, [arXiv:hep-ph/0607107 \[hep-ph\]](#).
- [42] F. R. Klinkhamer and R. Laterveer, “The Sphaleron at finite mixing angle,” *Z. Phys. C* **53** (1992) 247–252.
- [43] B. Kleihaus, J. Kunz, and Y. Brihaye, “The Electroweak sphaleron at physical mixing angle,” *Phys. Lett. B* **273** (1991) 100–104.
- [44] J. Kunz, B. Kleihaus, and Y. Brihaye, “Sphalerons at finite mixing angle,” *Phys. Rev. D* **46** (1992) 3587–3600.
- [45] A. Ahriche, “What is the criterion for a strong first order electroweak phase transition in singlet models?,” *Phys. Rev. D* **75** (2007) 083522, [arXiv:hep-ph/0701192 \[hep-ph\]](#).
- [46] P. H. Damgaard, A. Haarr, D. O’Connell, and A. Tranberg, “Effective Field Theory and Electroweak Baryogenesis in the Singlet-Extended Standard Model,” *JHEP* **02** (2016) 107, [arXiv:1512.01963 \[hep-ph\]](#).
- [47] D. Cutting, M. Hindmarsh, and D. J. Weir, “Vorticity, kinetic energy, and suppressed gravitational wave production in strong first order phase transitions,” [arXiv:1906.00480 \[hep-ph\]](#).
- [48] A. Alves, D. Gonalves, T. Ghosh, H.-K. Guo, and K. Sinha, “Di-Higgs Production in the  $4b$  Channel and Gravitational Wave Complementarity,” [arXiv:1909.05268 \[hep-ph\]](#).
- [49] F. L. Bezrukov, D. Levkov, C. Rebbi, V. A. Rubakov, and P. Tinyakov, “Semiclassical study of baryon and lepton number violation in high-energy electroweak collisions,” *Phys. Rev. D* **68** (2003) 036005, [arXiv:hep-ph/0304180 \[hep-ph\]](#).
- [50] F. L. Bezrukov, D. Levkov, C. Rebbi, V. A. Rubakov, and P. Tinyakov, “Suppression of baryon number violation in electroweak collisions: Numerical results,” *Phys. Lett. B* **574** (2003) 75–81, [arXiv:hep-ph/0305300 \[hep-ph\]](#).
- [51] A. Ringwald, “Electroweak instantons / sphalerons at VLHC?,” *Phys. Lett. B* **555** (2003) 227–237, [arXiv:hep-ph/0212099 \[hep-ph\]](#).
- [52] A. Ringwald, “An Upper bound on the total cross-section for electroweak baryon number violation,” *JHEP* **10** (2003) 008, [arXiv:hep-ph/0307034 \[hep-ph\]](#).
- [53] J. Ellis and K. Sakurai, “Search for Sphalerons in Proton-Proton Collisions,” *JHEP* **04** (2016) 086, [arXiv:1601.03654 \[hep-ph\]](#).
- [54] Y.-C. Qiu and S. H. H. Tye, “Role of Bloch Waves in baryon-number violating processes,” *Phys. Rev. D* **100** no. 3, (2019) 033006, [arXiv:1812.07181 \[hep-ph\]](#).
- [55] S. H. H. Tye and S. S. C. Wong, “Baryon Number Violating Scatterings in Laboratories,” *Phys. Rev. D* **96** no. 9, (2017) 093004, [arXiv:1710.07223 \[hep-ph\]](#).
- [56] J. Ellis, K. Sakurai, and M. Spannowsky, “Search for Sphalerons: IceCube vs. LHC,” *JHEP* **05** (2016) 085, [arXiv:1603.06573 \[hep-ph\]](#).
- [57] S. H. H. Tye and S. S. C. Wong, “Bloch Wave Function for the Periodic Sphaleron Potential and Unsuppressed Baryon and Lepton Number Violating Processes,” *Phys. Rev. D* **92** no. 4, (2015) 045005, [arXiv:1505.03690 \[hep-th\]](#).
- [58] S. Di Vita, G. Durieux, C. Grojean, J. Gu, Z. Liu, G. Panico, M. Riembau, and T. Vantalón, “A global view on the Higgs self-coupling at lepton colliders,” *JHEP* **02** (2018) 178, [arXiv:1711.03978 \[hep-ph\]](#).
- [59] T. Liu, K.-F. Lyu, J. Ren, and H. X. Zhu, “Probing the quartic Higgs boson self-interaction,” *Phys. Rev. D* **98** no. 9, (2018) 093004, [arXiv:1803.04359 \[hep-ph\]](#).
- [60] G. D. Moore, “Measuring the broken phase sphaleron rate nonperturbatively,” *Phys. Rev. D* **59** (1999) 014503, [arXiv:hep-ph/9805264 \[hep-ph\]](#).
- [61] J. O. Andersen, T. Gorda, A. Helset, L. Niemi, T. V. I. Tenkanen, A. Tranberg, A. Vuorinen, and D. J. Weir, “Nonperturbative Analysis of the Electroweak Phase Transition in the Two Higgs Doublet Model,” *Phys. Rev. Lett.* **121** no. 19, (2018) 191802, [arXiv:1711.09849 \[hep-ph\]](#).
- [62] T. Gorda, A. Helset, L. Niemi, T. V. I. Tenkanen, and D. J. Weir, “Three-dimensional effective theories for the two Higgs doublet model at high temperature,” *JHEP* **02** (2019) 081, [arXiv:1802.05056 \[hep-ph\]](#).
- [63] K. Kainulainen, V. Keus, L. Niemi, K. Rummukainen, T. V. I. Tenkanen, and V. Vaskonen, “On the validity of perturbative studies of the electroweak phase transition in the Two Higgs Doublet model,” *JHEP* **06** (2019) 075, [arXiv:1904.01329 \[hep-ph\]](#).
- [64] K. Farakos, K. Kajantie, K. Rummukainen, and M. E. Shaposhnikov, “3-D physics and the electroweak phase transition: Perturbation theory,” *Nucl. Phys. B* **425** (1994) 67–109, [arXiv:hep-ph/9404201 \[hep-ph\]](#).
- [65] K. Kajantie, M. Laine, K. Rummukainen, and M. E. Shaposhnikov, “Generic rules for high temperature dimensional reduction and their application to the standard model,” *Nucl. Phys. B* **458** (1996) 90–136, [arXiv:hep-ph/9508379 \[hep-ph\]](#).
- [66] J. M. No, “Large Gravitational Wave Background Signals in Electroweak Baryogenesis Scenarios,” *Phys. Rev. D* **84** (2011) 124025, [arXiv:1103.2159 \[hep-ph\]](#).
- [67] J. R. Espinosa, T. Konstandin, J. M. No, and G. Servant, “Energy Budget of Cosmological First-order Phase Transitions,” *JCAP* **1006** (2010) 028, [arXiv:1004.4187 \[hep-ph\]](#).
- [68] C. Caprini, R. Durrer, and G. Servant, “The stochastic gravitational wave background from turbulence and magnetic fields generated by a first-order phase transition,” *JCAP* **0912** (2009) 024, [arXiv:0909.0622 \[astro-ph.CO\]](#).
- [69] P. Binetruy, A. Bohe, C. Caprini, and J.-F. Dufaux, “Cosmological Backgrounds of Gravitational Waves and eLISA/NGO: Phase Transitions, Cosmic Strings and Other Sources,” *JCAP* **1206** (2012) 027, [arXiv:1201.0983 \[gr-qc\]](#).
- [70] K. Fuyuto and E. Senaha, “Improved sphaleron decoupling condition and the Higgs coupling constants in the real singlet-extended standard model,” *Phys. Rev.*

**D90** no. 1, (2014) 015015, [arXiv:1406.0433 \[hep-ph\]](#).  
[71] W. H. Press, S. A. Teukolsky, W. T. Vetterling, and  
B. P. Flannery, *Numerical Recipes 3rd Edition: The Art*

*of Scientific Computing*. Cambridge University Press,  
New York, NY, USA, 3 ed., 2007.